Applied Catalysis A: General 506 (2015) 173–179

Contents lists available at ScienceDirect

Applied Catalysis A: General

journal homepage: www.elsevier.com/locate/apcata

Mo Schiff base-tungstate ionic hybrid with enhanced heterogeneous catalytic activity for epoxidation reactions

Weizheng Fan[b], Yan Leng[a,*], Jian Liu[a], Pingping Jiang[a], Jiwei Zhao[a]

[a] The Key Laboratory of Food Colloids and Biotechnology, Ministry of Education, School of Chemical and Material Engineering, Jiangnan University, Wuxi 214122, China
[b] School of Pharmaceutical Science, Jiangnan University, Wuxi 214122, China

ARTICLE INFO

Article history:
Received 13 May 2015
Received in revised form 7 September 2015
Accepted 9 September 2015
Available online 12 September 2015

Keywords:
Mo Schiff base
Epoxidation
Heterogeneous catalysis
Tungstate
Ionic liquid

ABSTRACT

A novel metal Schiff base-tungstate ionic hybrid (Mo–MimAM–WO_4) was prepared by anion-exchange of Mo Schiff base functionalized imidazole ionic liquid with sodium tungstate. The resulting hybrid catalyst was fully characterized by ^{1}H NMR, FT-IR, XRD, SEM, TGA, and XPS, and its catalytic activity was studied for the epoxidation of alkenes using aqueous H_2O_2 as the oxidant. The catalyst was found to be highly efficient and showed higher catalytic activity than its corresponding homogeneous and heterogeneous analogues Mo–MimAM and Na_2WO_4. After reaction, the catalyst can be easily recovered by filtration and reused for the next run. The synergistic effect between Mo Schiff base complex and tungstate is revealed to be responsible for the catalyst's excellent performance in epoxidation.

1. Introduction

Epoxides are well known as one of the most valuable building blocks that can be used as intermediates and precursors for chemical production [1,2]. The oxidation of alkenes with aqueous hydrogen peroxide (H_2O_2) is very attractive from the viewpoint of industrial production and synthetic organic chemistry, since aqueous H_2O_2 is cheap, environmentally clean and easy to handle [3–5]. Over the past decades, several transition metals such as molybdenum [6–11], tungsten [12–16], vanadium [17,18], manganese [19,20], titanium [21–23], iron [24,25], *etc.* have been widely used as homogenous catalysts in oxidation systems based on aqueous H_2O_2. Among them, molybdenum and tungsten-based catalyst systems are promising for epoxidation of alkenes owing to their high efficiency and selectivity.

Transition metal Schiff base complexes are an important class of redox catalysts because of that the metal-organic framework is suitable for the construction of a highly functionalized coordination site, which may provide an opportunity to further enhance the catalytic activity [26,27]. Some of metal Schiff base complexes [6,7], particularly molybdenum Schiff base complexes have shown very interesting catalytic properties in epoxidation of alkenes [28,29]. However, most of these catalytic systems are homogeneous, suffering from problems associated with the separation and recovery of the catalysts and inevitable metal contamination of the products. To overcome these problems, heterogeneous catalysts have been prepared by immobilizing the metal Schiff base complexes onto organic polymers [8–10] or inorganic materials such as grapheme [23], alumina [21], silica [17] and so on. For example, Jia [30] have synthesized mesoporous MCM-41 materials modified with oxodiperoxo molybdenum complexes and found that these materials are active in the epoxidation of cyclooctene. We recently prepared a novel kind of POSS-bridged Mo Schiff base hybrids and used it as efficient heterogeneous catalysts for epoxidation of alkenes with tert-butyl hydroperoxide (TBHP) [10]. Though heterogeneous catalysis was achieved in those cases, most of them still bear some drawbacks like the slow reaction rate, leaching of active species, or need expensive oxidant. Therefore, it is necessary to develop new strategies to generate heterogeneous metal Schiff base catalysts.

Task specific ionic liquids (TSILs), in which functional groups are covalently tethered to the cation or anion (or both) of the ILs, have increased attention over the last few years as it is possible to form any specific composition depending upon user's need of the desired physical, chemical and catalytic properties [31–33]. An interesting example of TSILs is focused on the incorporation of organometallic groups into a branch appended to the cation of ILs [34,35]. For example, Tan and co-workers [36,37] have shown that

* Corresponding author. Fax: +86 510 85917763.
E-mail address: lengyan1114@126.com (Y. Leng).

http://dx.doi.org/10.1016/j.apcata.2015.09.011
0926-860X/

ILs complexes functionalized by chiral salen Mn(III) were efficient and recyclable catalysts for enantioselective epoxidation of styrene. Further, taking into account that the combination of IL cations with metal-containing inorganic anions can cause the formation of ionic hybrids with high melting point and insolubility that are emerging to be very important in catalysis [38,39]. Accordingly, we think that it is rational to prepare a composite catalyst by pairing metal Schiff base functionalized IL cations with metal-containing inorganic anions. The resulting composite may be a novel heterogeneous catalyst for epoxidation of alkenes with H_2O_2.

Herein, we demonstrate a novel metal Schiff base-tungstate ionic hybrid whereby molybdenum (Mo) Schiff base and tungstate (WO_4^{2-}) were attached to IL cation and anion, respectively. It was fully characterized by ^{1}H NMR, FT-IR, XRD, SEM, TGA, and XPS, and used as a highly efficient heterogeneous catalyst in the epoxidation of alkenes with H_2O_2, showing a better catalytic activity than the Schiff base metal complex or WO_4^{2-} along.

2. Experimental

2.1. Reagents and analysis

All chemicals were analytical grade (purity > 99%) and used as received. FT-IR spectra were recorded on a Nicolet 360 FT-IR instrument (KBr discs) in the 4,000–400 cm^{-1} region. ^{1}H NMR spectra were measured with a Bruker DPX 400 spectrometer at ambient temperature in D_2O using TMS as internal reference. TG analysis was carried out with a STA409 instrument in dry air at a heating rate of 10 °C/min. SEM image was performed on a HITACHI S-4800 field-emission scanning electron microscope. XRD patterns were collected on the Bruker D8 Advance powder diffractometer using Ni-filtered Cu/Kα radiation source at 40 kV and 20 mA, from 5–80° with a scan rate of 4°/min. The metal species were detected by X-ray photoelectron spectroscopy (XPS, Thermo ESCALAB 250 Xi). The spectra were recorded with Al Kα line as the excitation source ($h\nu$ = 1486.6 eV). The binding energy (B.E.) values were referenced to the C 1s peak of contaminant carbon at 284.8 eV. The amount of leached Mo species in the filtrate was measured using a Jarrell-Ash 1100 ICP-AES spectrometer. The CHN elemental analysis was performed on an elemental analyzer Vario EL cube.

2.2. Preparation of catalysts

2.2.1. Synthesis of [3-aminoethyl-1-methylimidazolium]Br (MimAM)

MimAM was prepared as following: In detail, *N*-methylimidazole (8.2 g, 0.1 mol) and 2-bromoethylaminehydrobromide (20.5 g, 0.1 mol) were dissolved in 50 mL absolute ethanol at 80 °C for 48 h under nitrogen atmosphere with reflux and stirring. On completion, solvent was removed by distillation, and the residue was washed with ethyl acetate for 3 times to afford the IL precursor MimAM·HBr. KOH was added into the aqueous solution of the above solid for neutralization, followed by the evaporation under vacuum. Methanol (20 mL) and $CHCl_3$ (2 mL) were added into the resulting mixture with the appearance of precipitated salts. After filtration, the filtrate was evaporated to give the MimAM product as yellow oil. ^{1}H NMR (400 MHz, D_2O, TMS) δ(ppm) = 3.47 (m, 2H, —CH_2), 4.58 (m, 2H, —CH_2), 5.40 (dd, 1H, —CH), 5.81 (dd, 1H, —CH), 7.13 (m, 1H, —CH), 7.66 (s, 1H, —CH), 7.81 (s, 1H, —CH), 9.18 (s, 1H, —CH). CHN elemental analysis for MimAM (by the mass percentage): C 34.97%; N 20.39%; H 5.87%. Found: C 34.58%; N 20.25%; H 5.96%.

2.2.2. Synthesis of [$MoO_2(acac)_2$]

Molybdenyl acetylacetonate [$MoO_2(acac)_2$] was prepared according to previous literature [40] with about 51% yield.

2.2.3. Synthesis of Mo–MimAM

Mo–MimAM was prepared according to previous literature [41]. In detail, MimAM (1.21 g, 6 mmol) dissolved in anhydrous ethanol (10 mL) was added dropwise into the ethanol (10 mL) solution of [$MoO_2(acac)_2$] (0.98 g, 3 mmol) with vigorous stirring, the resulting mixture was refluxed at room temperature for 24 h under a nitrogen atmosphere. The formed light-blue solid precipitate was filtered off and washed thoroughly by H_2O and ethanol, and dried under vacuum. CHN elemental analysis for Mo–MimAM (by the mass percentage): C 43.87%; N 13.95%; H 5.02%. Found: C 44.11 %; N 13.37 %; H 5.94 %.

2.2.4. Synthesis of Mo–MimAM–WO_4

The obtained Mo-MimAM (1.5 g, 2 mmol) was dissolved in 30 mL ethanol in a 100 mL round bottom flask. Then, an aqueous solution of $Na_2WO_4{\cdot}2H_2O$ (1.0 g, 3 mmol) was added to the solution of Mo–MimAM, followed by the stirring of the mixture for 24 h at 80 °C. The white precipitate Mo–MimAM–WO_4 was filtered and washed thoroughly with H_2O and ethanol, and dried under vacuum. CHN elemental analysis for Mo–MimAM–WO_4 (by the mass percentage): C 26.93%; N 7.85%; H 3.95%. Found: C 26.65 %; N 7.8 %; H 4.04 %.

2.3. Catalytic tests

Cyclooctene (1 mmol), CH_3CN (5 mL), and catalyst Mo–MimAM–WO_4 (10 mg) were added into a 25 mL round bottom flask. The reaction system was heated to 60 °C with vigorous stirring, then, and the aqueous H_2O_2 (30 wt.%, 2.5 mmol) was added dropwise into the reaction mixture within 10 min. After that, the reaction was stirred for another 4 h at 60 °C. After the reaction, the catalyst was filtered off, washed with ethanol and dried at 80 °C for another run. The product mixture was analyzed by gas chromatography (GC) (SP-6890A) equipped with a FID detector and a capillary column (SE-54 30 m × 0.32 mm × 0.3 m). Calibration area normalization method was used to quantify the products, and each reaction mixture sample was detected five times to take the average. Notably, the deviation of the five measurements is less than 2%.

3. Results and discussion

3.1. Catalyst preparation and characterization

The synthetic route for Mo–MimAM–WO_4 is shown in Scheme 1. The organic-molybdenum ionic complex abbreviated as Mo–MimAM was prepared by covalent binding amino functionalized IL and $MoO_2(acac)_2$. Then, WO_4^{2-} species was introduced by anion-exchange of Mo–MimAM with Na_2WO_4 to give the final catalyst Mo–MimAM–WO_4, which was fully characterized by FT-IR, XRD, SEM, TG, XPS, and CHN elemental analysis. The CHN elemental analysis for Mo–MimAM–WO_4 showed 26.65% for the weight percentage of C, 7.8% for N, and 4.04% for H, which is very near to the theoretical values of C: 26.93%, N: 7.85%, and H: 3.95%. Moreover, the TG profile (Fig. 1) indicates that Mo-MimAM-WO_4 was quite stable up to 290 °C, the total weight loss of about 45% was somewhat corresponding to the decomposition of both organic and inorganic moieties of the catalyst into individual oxides (MoO_3 and WO_3) (calculated weight loss: 42%).

Fig. 2 compares the FT-IR spectrum of Mo–MimAM–WO_4 with those of [$MoO_2(acac)_2$], Na_2WO_4, and Mo–MimAM. [$MoO_2(acac)_2$]

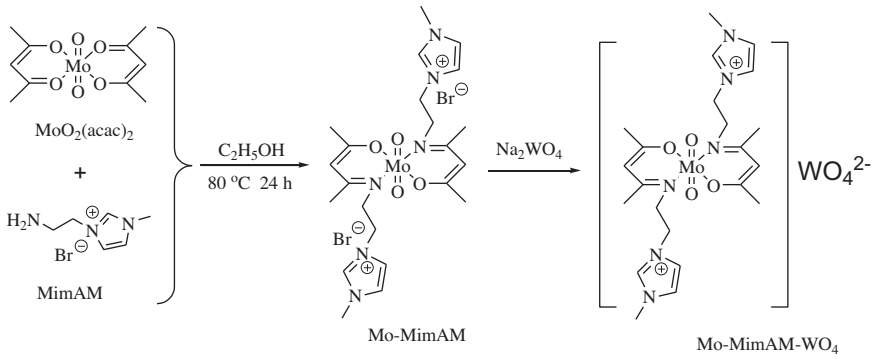

Scheme 1. Preparation of Mo–MimAM–WO_4 ionic hybrid catalyst.

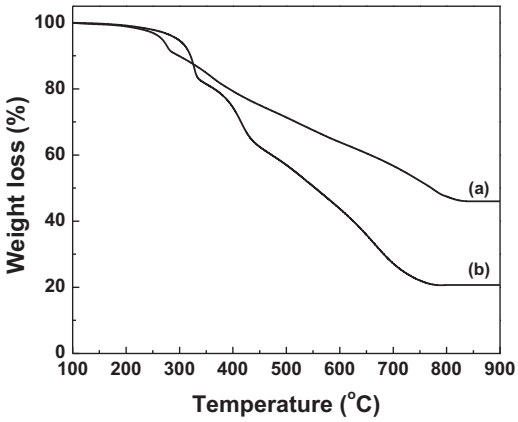

Fig. 1. TG curves of catalysts (a) Mo–MimAM–WO_4, and (b) Mo–MimAM.

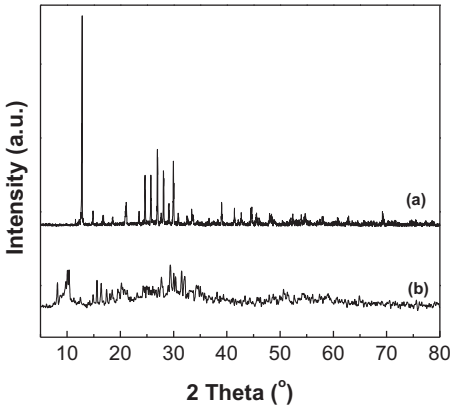

Fig. 3. XRD patterns of (a) Na_2WO_4 and (b) Mo–MimAM–WO_4.

presents two strong characteristic bands at 935 and 904 cm^{-1} that are attributed to the stretching vibration of $(MoO_2)_{asym}$ and $(MoO_2)_{sym}$, respectively (Fig. 2, curve a), and Na_2WO_4 shows two strong bands at 834 and 857 cm^{-1} that are attributed to the stretching vibration of the W—O and W=O, respectively (Fig. 2, curve b). The IR spectrum of Mo–MimAM shows the characteristic peaks at 947, 917, and 843 cm^{-1}, assignable to the vibrations of $(MoO_2)_{asym}$, $(MoO_2)_{sym}$, and Mo—O, respectively (Fig. 2, curve c). For the developed hybrid catalyst Mo–MimAM–WO_4 (Fig. 2, curve d), the above peaks appeared distinctively, and the slight shifts of the above bands for Mo–MimAM–WO_4 result from the strong ionic interactions between IL cations and WO_4^{2-} anions.

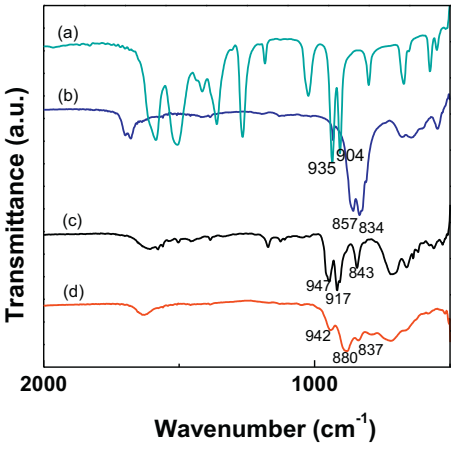

Fig. 2. FT-IR spectra of catalysts (a) $MoO_2(acac)_2$, (b) Na_2WO_4, (c) Mo–MimAM, and (d) Mo–MimAM–WO_4.

Thus, the observed phenomenon implies the formation of a new organometallic-tungstate ionic hybrid via ionic linkage between the organic cation and the WO_4^{2-} anion.

The XRD pattern in Fig. 3, curve a displays the featured diffraction peaks for the orthorhombic phase of Na_2WO_4. However, the intensity of all these peaks declined in the case of Mo–MimAM–WO_4. It is thus suggested that the developed ionic hybrid catalyst is almost amorphous in nature. Indeed, the SEM image for Mo–MimAM–WO_4 (Fig. 4) shows an amorphous structure with rough surface.

3.2. Catalytic activity in the epoxidation reaction

The catalytic performance of the catalyst Mo–MimAM–WO_4 and comparison with various reference catalysts were first assessed in the epoxidation of cyclooctene using H_2O_2 as oxidant at 60 °C in CH_3CN, the results are listed in Table 1. It can be seen that the reaction did not proceed at all in the absence of catalyst (Table 1, Entry 1). The pure [$MoO_2(acac)_2$] (Table 1, Entry 2) showed a conversion of 83% with 100% selectivity, but it dissolved in the reaction medium to give homogeneous systems. After the combination of $MoO_2(acac)_2$ and IL MimAM, the resulting Mo–MimAM caused a heterogeneous reaction system, with a significant decrease of conversion down to 54% (Table 1, Entry 3). Additionally, Na_2WO_4 was partially soluble in the reaction media, but showed very low conversion of 2% (Table 1, Entry 4). In contrast, the hybrid catalyst Mo–MimAM–WO_4 obtained by combining Mo–MimAM and Na_2WO_4 caused a liquid-solid heterogeneous epoxidation system, and offered a much higher conversion of 99% than its precursors did (Table 1, entry 5). The above comparison results imply that there might generate some synergistic effects

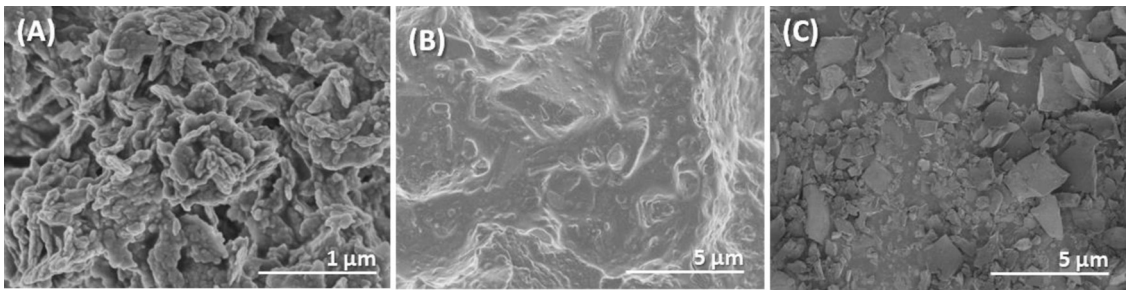

Fig. 4. SEM images of (A) Mo–MimAM, (B) Mo–MimAM–WO_4, and (C) Na_2WO_4.

Table 1
Catalytic performances of various catalysts for the epoxidation of cyclooctene using H_2O_2.[a]

Entry	Catalyst	Solubility in reaction	X[b] (%)	S[c] (%)
1[d]	None	–	n.d.	n.d.
2	$MoO_2(acac)_2$	Soluble	83	100
3	Mo–MimAM	Insoluble	54	100
4	Na_2WO_4	Partially soluble	2	100
5	Mo–MimAM–WO_4	Insoluble	99	100

[a] Reaction conditions: catalyst (0.01 g), cyclooctene (1 mmol), H_2O_2 (30%, 2.5 mmol), CH_3CN (5 mL), 60 °C, 4 h.
[b] Conversion.
[c] Selectivity were determined by GC.
[d] The reaction was performed in the absence of catalyst, and the conversion was too low to be determined (abbreviated as "n.d.").

between Mo–MimAM and WO_4^{2-} that endows the catalyst with superior catalytic activity for epoxidation reaction. The catalytic activity and selectivity of Mo–MimAM–WO_4 for the epoxidation of cyclooctene are higher or comparable to those of the previously reported heterogeneous catalysts, such as supported tungsten oxide [42], peroxometalate-based polymer-mobilized ionic liquid phase (PIILP) catalyst [43] and CuO nanoclusters coated with mesoporous SiO_2 [44], as well as the homogeneous vanadium complex [45].

3.3. Influences of reaction conditions

The influences of the reaction conditions on the epoxidation of cyclooctene with H_2O_2 over Mo–MimAM–WO_4 are shown in Fig. 5, including the reaction temperature, catalyst amount, reaction time, and molar ratio of H_2O_2 to cyclooctene. In all cases, the selectivity of epoxidation product was always 100%. It can be seen that the increase of the reaction temperature from 40 °C to 70 °C led to a remarkable increase in the conversion of cyclooctene. However, at a higher temperature 80 °C, the drastic decrease of the conversion was observed (Fig. 5A), mostly due to the more drastic self-decomposition of H_2O_2. Fig. 5B displays the effect of the catalyst amount on the conversion of cyclooctene. When the amount of catalyst was increased up to 0.01 g, the maximum conversion of 99% was achieved, a further increase of the catalyst amount reversely caused a slight decrease of the cyclooctene conversion, which may result from the deep oxidation of epoxidation product with more catalyst. The effect of the reaction time (Fig. 5C) and the molar ratio of H_2O_2 to cyclooctene (Fig. 5D) on the epoxidation of cyclooctene were also investigated, and the best experimental condition is 4 h of reaction time and 2.5:1 of H_2O_2/cyclooctene molar ratio, providing a conversion of 99% and a selectivity of 100%. Theoretically, the molar ratio of H_2O_2 to cyclooctene for the epoxidation reaction is 1:1, the H_2O_2 needed for the highest conversion was about 2.5 times as high as its stoichiometry, which could be attributed to the self-decomposition of H_2O_2 [46–48].

3.4. Epoxidation of various substrates over catalysts Mo–MimAM–WO_4 and Mo-MimAM

We assessed the catalytic activity of Mo–MimAM–WO_4 and Mo–MimAM under the described reaction conditions, using a series of various types of alkenes. The results are summarized in Table 2. It can be seen that heterogeneous catalyst Mo–MimAM–WO_4 shows much higher catalytic activity than that of Mo–MimAM in the majority of cases. These results further confirm the positive synergistic effect between Mo–MimAM and WO42$^-$ for epoxidation reactions. Moreover, cyclooctene, cyclohexene, and 3-hexan-1-ol with inner double bonds exhibit higher activities in comparison with 1-hexene and 1-octene which contain terminal double bonds.

3.5. Understanding of the catalytic behavior of Mo–MimAM–WO_4

Fig. 6(A) and (B) display the XPS spectra of the Na_2WO_4, Mo–MimAM, and Mo–MimAM–WO_4. As can be seen, the W 4f spectrum of Na_2WO_4 shows a spin-doublet peak with the binding energy of $4f_{7/2}$ and $4f_{5/2}$ at 35.2 and 37.3 eV, respectively, corresponding to the W^{6+} oxidation state, and the doublet Mo $3d_{5/2}$ and $3d_{3/2}$ peak at 231.3 and 234.5 eV is attributed to typical Mo^{6+} oxidation state. In the case of Mo–MimAM–WO_4, both W 4f and Mo 3d peaks appeared in the XPS spectra, suggesting the existence of two types of metal centres on the catalyst Mo–MimAM–WO_4. Furthermore, the position of the bands for W 4f and Mo 3d shifted to higher binding energy and the intensity of which decreased. This observation indicates the formation of new chemical microenvironment around Mo and W species by the synergistic effects between Mo–MimAM and WO_4^{2-}.

Further insights into Mo–MimAM–WO_4 catalyzed epoxidation was gained by the IR measurement of the Mo–MimAM–WO_4 after reacting with 30% H_2O_2 in CH_3CN at 60 °C for 10 min, which mimics the practical reaction but in the absence of alkene substrates, and the FT-IR spectra of H_2O_2 treated and fresh Mo–MimAM–WO_4 are illustrated in Fig. 7. On treatment with H_2O_2, the ν(Mo=O) and ν(W=O) bands at 942, and 880 cm^{-1} shifted to lower wavenumber in the spectrum for Mo–MimAM–WO_4, and two new distinct peaks at 620 and 540 cm^{-1} occurred. The new vibrations can be attributed to the peroxo-oxygen band ν(O—O) in Mo(O_2) and WO_4 species, respectively, which have been known as the active species for H_2O_2-based epoxidations [41,49,50]. The recovered catalyst from the reacted mixture returned to its original structure (Fig. 7, curve c). Therefore, the above results indicate that both peroxo–W and peroxo–Mo species are the possible intermediate active species, which may directly associate with the high activity and selectivity of Mo–MimAM–WO_4 for the epoxidation of alkenes.

3.6. Catalyst reusability

Further experiments were conducted to examine the recyclability and reusability of the Mo–MimAM–WO_4 in the epoxidation

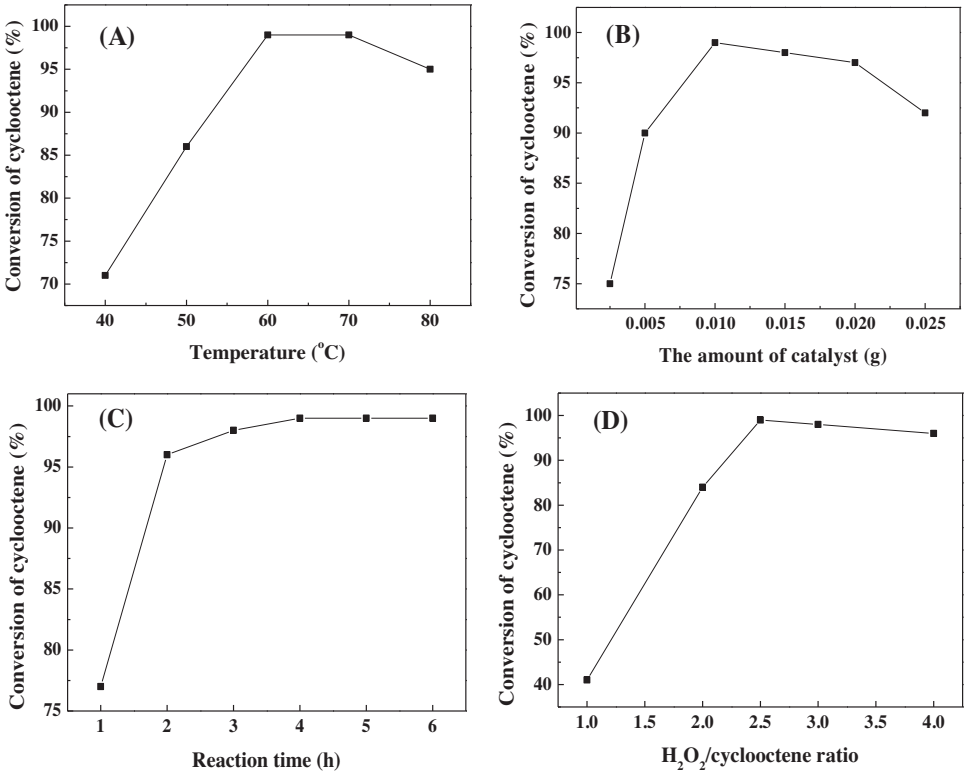

Fig. 5. Influences of reaction conditions on epoxidation of cyclooctene with H_2O_2 over catalyst Mo–MimAM–WO_4: (A) reaction temperature, (B) the amount of catalyst, (C) reaction time, and (D) the molar ratio of H_2O_2 to cyclooctene. For each figure there is a specific parameter changed, and the selectivity in all cases is 100%.

Table 2
Epoxidation of various substrates over catalysts Mo–MimAM–WO_4 and Mo–MimAM.[a]

Entry	Substrate	Product	*t* (h)	X^b (%) Mo–MimAM–WO_4	S^c (%)	X^b (%) Mo–MimAM	S^c (%)
1			4	99	100	54	100
2			12	65	62	53	30
3	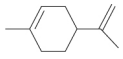	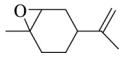	12	49	61	40	49
4	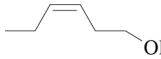	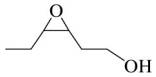	12	80	100	28	100
5	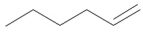	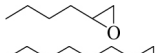	12	27	100	10	100
6	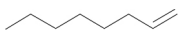	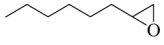	12	19	100	6	100

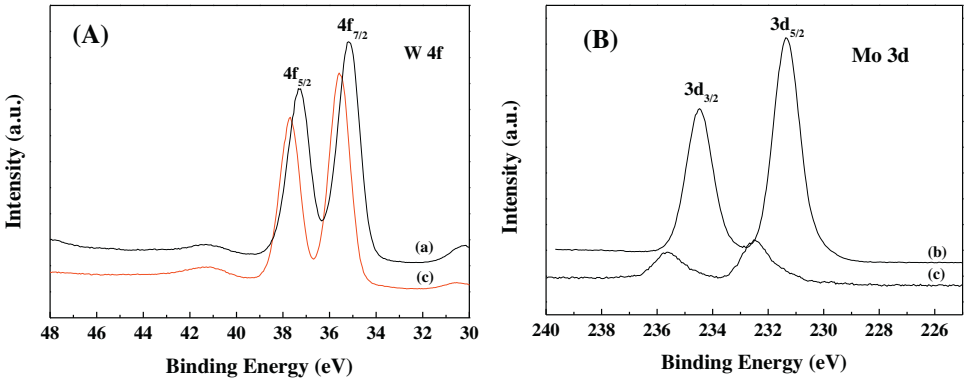

Fig. 6. XPS spectra of (a) Na_2WO_4, (b) Mo–MimAM, and (c) Mo–MimAM–WO_4.

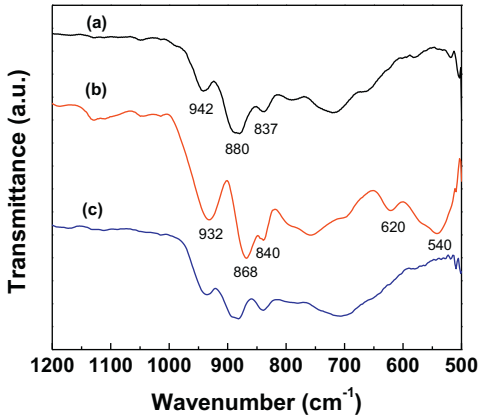

Fig. 7. FT-IR spectra of (a) fresh Mo–MimAM–WO_4, (b) H_2O_2 treated Mo–MimAM–WO_4, and (c) three times reused Mo–MimAM–WO_4.

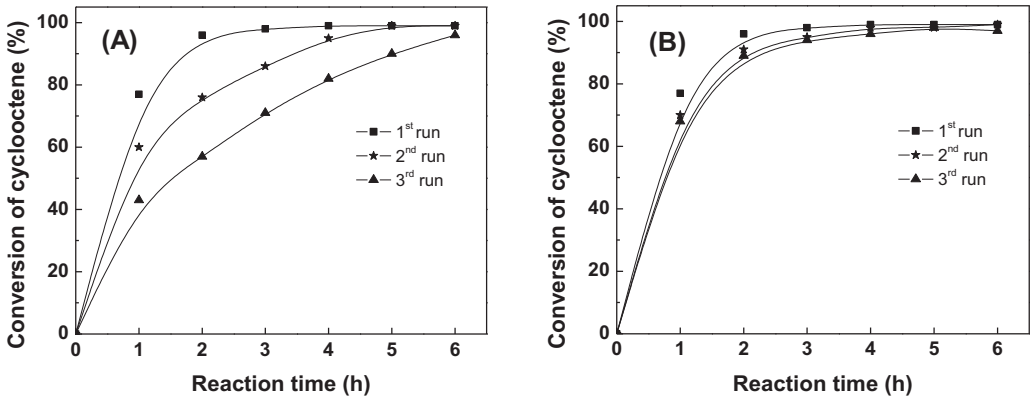

Fig. 8. (A) Catalytic reusability of Mo–MimAM–WO_4 for the epoxidation of cyclooctene with H_2O_2. (B) Catalytic reusability of Mo–MimAM–WO_4 for the epoxidation of cyclooctene with H_2O_2 with the addition of fresh catalyst to resume the constant catalyst amount of 0.01 g. Reaction conditions: cyclooctene (1 mmol), H_2O_2 (30%, 2.5 mmol), CH_3CN (5 mL), 60 °C.

of alkenes by using cyclooctene as a model substrate. After the reaction, the catalyst was recovered from the reaction mixture by filtration, washed with ethanol, dried and reused for the next run without adding any fresh catalyst. Fig. 8(A) gives the three-run catalyst recycling results for epoxidation of cyclooctene with H_2O_2. A selectivity of 100% could always be obtained, and high conversions above 95% were achieved in the second and third run with a slightly longer reaction time of 6 h. However, the reaction rate decreased gradually over the three run tests. The result of ICP-AES elemental analysis for the reacted filtrate shows that about 4.9 wt.% Mo and 2.3 wt.% W in the catalyst had leached into the reaction media. Consequently, a hot-filtration experiment was carried out. Initially, the mixture of cyclooctene, catalyst Mo–MimAM–WO_4, and H_2O_2 in acetonitrile was stirred at 60 °C for 1 h. The cyclooctene conversion of 76.3% was obtained at the reaction time of 1 h. Then, the catalyst was removed and the reaction proceeded for another 4 h with the homogeneous filtrate, the conversion was increased slightly to 80.9%. This result suggests that such a small amount leaching of Mo and W species did not play a key role in the decrease of catalytic activities. Notably, the weight loss in the operation for recovering the catalyst is unavoidable (about 77 wt% of the catalyst was recovered after the first run), when a small amount of the fresh catalyst was added into the recovered one to resume the constant catalyst amount of 0.01 g as in the first run, the catalyst showed a relative steady conversion of cyclooctene (Fig. 8B). The above results indicate that the decrease of the catalytic activity is mostly attributed to the weight loss in the operation for recovering the catalyst and the catalyst's leaching during the reaction.

4. Conclusions

In summary, we have successfully prepared a novel metal Schiff base-tungstate ionic hybrid Mo–MimAM–WO_4 by anion-exchange of Mo Schiff base functionalized IL Mo–MimAM with Na_2WO_4. The resulting ionic hybrid containing two types of metal active centers Mo and W was proved to be an effective and recyclable catalyst for heterogeneous epoxidation of alkenes with H_2O_2, exhibiting higher catalytic activity than those of its precursors Mo–MimAM and Na_2WO_4. The overall superior catalytic activity of the catalyst associates with the synergistic effect between Mo Schiff base and WO_4^{2-} species that result in the improved redox property of the hybrid catalyst.

Acknowledgements

The authors thank the National Natural Science Foundation of China (No. 21206052) and MOE & SAFEA for the 111 Project (No. B13025).

References

[1] O.A. Wong, Y. Shi, Chem. Rev. 108 (2008) 3958–3987.
[2] Q. Gao, S. Wang, Y. Tang, C. Giordano, Chem. Commun. 48 (2012) 260–262.
[3] G.D. Faveri, G. Ilyashenko, M. Watkinson, Chem. Soc. Rev. 40 (2011) 1722–1760.
[4] Z. Xi, N. Zhou, Y. Sun, K. Li, Science 292 (2001) 1139–1141.
[5] K. Kamata, K. Yonehara, Y. Sumida, K. Yamaguchi, S. Hikichi, N. Mizuno, Science 300 (2003) 964–966.

[6] M. Herbert, E. Alvarez, D.J. Cole-Hamilton, F. Montilla, A.N. Galindo, Chem. Commun. 46 (2010) 5933–5935.
[7] S. Krackl, A. Company, S. Enthaler, M. Driess, ChemCatChem 3 (2011) 1186–1192.
[8] K.C. Gupta, A.K. Sutar, C.C. Lin, Coord. Chem. Rev. 253 (2009) 1926–1946.
[9] J. Moreno, J. Iglesias, J.A. Melero, D.C. Sherrington, J. Mater. Chem. 21 (2011) 6725–6735.
[10] Y. Leng, J. Liu, C.J. Zhang, P. Jiang, Catal. Sci. Technol. 4 (2014) 997–1004.
[11] N.L.D. Filho, F.C.M. Portugal, J.M.F. Nogueira, P. Branda, V. Feílix, P.D. Vaz, L.F. Veiros, M.J.V.D. Brito, M.J. Calhorda, Organometallics 31 (2012) 4495–4503.
[12] K. Kamata, K. Yonehara, Y. Sumida, K. Hirata, S. Nojima, N. Mizuno, Angew. Chem. 123 (2011) 12268–12272.
[13] S.P. Maradur, C. Jo, D.H. Choi, K. Kim, R. Ryoo, ChemCatChem 3 (2011) 1435–1438.
[14] C. Wang, H. Yamamoto, J. Am. Chem. Soc. 136 (2014) 1222–1225.
[15] C. Hammond, J. Straus, M. Righettoni, S.E. Pratsinis, I. Hermans, ACS Catal. 3 (2013) 321–327.
[16] R. Ishimoto, K. Kamata, N. Mizuno, Angew. Chem. 124 (2012) 4740–4743.
[17] A. Held, J. Kowalska-Kus, A. Łapinski, K. Nowinska, J. Catal. 306 (2013) 1–10.
[18] G.C. Behera, K.M. Parida, Appl. Cata. A: Gen. 464–465 (2013) 364–373.
[19] F. Song, C. Wang, J.M. Falkowski, L. Ma, W. Lin, J. Am. Chem. Soc. 132 (2010) 15390–15398.
[20] N.J. Schoenfeldt, Z. Ni, A.W. Korinda, R.J. Meyer, J.M. Notestein, J. Am. Chem. Soc. 133 (2011) 18684–18695.
[21] P.J. Cordeiro, T.D. Tilley, ACS Catal. 1 (2011) 455–467.
[22] T.D. Baerdemaeker, B. Steenackers, D.D. Vos, Chem. Commun. 49 (2013) 7474–7476.
[23] J. Hu, J. Phys. Chem. C 117 (2013) 16005–16011.
[24] O. Cusso, I. Garcia-Bosch, X. Ribas, J. Lloret-Fillol, M. Costas, J. Am. Chem. Soc. 135 (2013) 14871–14878.
[25] T. Niwa, M. Nakada, J. Am. Chem. Soc. 134 (2012) 13538–13541.
[26] K.C. Gupta, A.K. Sutar, Coord. Chem. Rev. 252 (2008) 1420–1450.
[27] S. Verma, M. Nandi, A. Modak, S.L. Jain, A. Bhaumik, Adv. Synth. Catal. 353 (2011) 1897–1902.
[28] M. Herbert, E. Álvarez, D.J. Cole-Hamilton, F. Montilla, A. Galindo, Chem. Commun. 46 (2010) 5933–5935.
[29] A. Schmidt, N. Grover, T.K. Zimmermann, L. Graser, M. Cokoja, A. Pöthig, F.E. Kühn, J. Catal. 319 (2014) 119–126.
[30] M. Jia, A. Seifert, W.R. Thiel, Chem. Mater. 15 (2003) 2174–2180.
[31] G. Liu, M. Hou, J. Song, T. Jiang, H. Fan, Z. Zhang, B. Han, Green Chem. 12 (2010) 65–69.
[32] B. Wu, Y. Kuang, Y. Zhang, X. Zhang, J. Chen, J. Mater. Chem. 22 (2012) 13085–13090.
[33] A. Pourjavadi, S.H. Hosseini, M. Doulabi, S.M. Fakoorpoor, F. Seidi, ACS Catal. 2012 (2012) 1259–1266.
[34] Q. Yao, Angew. Chem. Int. Ed. 42 (2003) 3392–3395.
[35] C. Baleizao, B. Gigante, H. Garcia, A. Corma, Tetrahedron Lett. 44 (2004) 6813–6817.
[36] R. Tan, D. Yin, N. Yu, Y. Jin, H. Zhao, D. Yin, J. Catal. 255 (2) (2008) 287–295.
[37] R. Tan, D. Yin, N. Yu, H. Zhao, D. Yin, J. Catal. 263 (2) (2009) 284–291.
[38] A. Pourjavadi, S.H. Hosseini, F.M. Moghaddam, B.K. Foroushani, C. Bennett, Tungstate based poly(ionic liquid) entrapped magnetic nanoparticles: a robust oxidation catalyst, Green Chem. 15 (2013) 2913–2919.
[39] Y. Leng, J. Wu, P. Jiang, J. Wang, Catal. Sci. Technol. 4 (2014) 1293–1300.
[40] G.J.J. Chen, J.W. Mcdonald, W.E. Newton, Mech. Implic. Inorg. Chem. 15 (1976) 2612–2615.
[41] P. Borah, X. Ma, K.T. Nguyen, Y. Zhao, Angew. Chem. Int. Ed. 51 (2012) 7756–7761.
[42] K. Kamata, K. Yonehara, Y. Sumida, K. Hirata, S. Nojima, N. Mizuno, Angew. Chem. Int. Ed. 50 (2011) 12062–12066.
[43] S. Doherty, J.G. Knight, J.R. Ellison, D. Weekes, R.W. Harrington, C. Hardacre, H. Manyar, Green Chem. 14 (2012) 925–929.
[44] C. Chen, J. Qu, C. Cao, F. Niu, W. Song, J. Mater. Chem. 21 (2011) 5774–5779.
[45] G. Grivani, A.D. Khalaji, V. Tahmasebi, K. Gotoh, H. Ishida, Polyhedron 31 (2012) 265–271.
[46] Y. Leng, H. Ge, C. Zhou, J. Wang, Chem. Eng. J. 145 (2008) 335–339.
[47] Y. Leng, J. Liu, P. Jiang, J. Wang, Chem. Eng. J. 239 (2014) 1–7.
[48] Y. Leng, J. Liu, P. Jiang, J. Wang, RSC Adv. 2 (2012) 11653–11656.
[49] D.C. Duncan, R.C. Chambers, E. Hecht, C.L. Hill, J. Am. Chem. Soc. 117 (1995) 681–691.
[50] J.J. Boruah, S.P. Das, S.R. Ankireddy, S.R. Gogoi, N.S. Islam, Green Chem. 15 (2013) 2944–2959.